[CANCER RESEARCH 64, 8585–8594, December 1, 2004]

Identification and Testing of a Gene Expression Signature of Invasive Carcinoma Cells within Primary Mammary Tumors

Weigang Wang, Sumanta Goswami, Kyle Lapidus, Amber L. Wells, Jeffrey B. Wyckoff, Erik Sahai, Robert H. Singer, Jeffrey E. Segall, and John S. Condeelis

Department of Anatomy and Structural Biology, Albert Einstein College of Medicine, Bronx, New York

ABSTRACT

We subjected cells collected using an *in vivo* invasion assay to cDNA microarray analysis to identify the gene expression profile of invasive carcinoma cells in primary mammary tumors. Expression of genes involved in cell division, survival, and cell motility were most dramatically changed in invasive cells indicating a population that is neither dividing nor apoptotic but intensely motile. In particular, the genes coding for the minimum motility machine that regulates β-actin polymerization at the leading edge and, therefore, the motility and chemotaxis of carcinoma cells, were dramatically up-regulated. However, ZBP1, which restricts the localization of β-actin, the substrate for the minimum motility machine, was down-regulated. This pattern of expression implicated ZBP1 as a suppressor of invasion. Reexpression of ZBP1 in metastatic cells with otherwise low levels of ZBP1 reestablished normal patterns of β-actin mRNA targeting and suppressed chemotaxis and invasion in primary tumors. ZBP1 reexpression also inhibited metastasis from tumors. These experiments support the involvement in metastasis of the pathways identified in invasive cells, which are regulated by ZBP1.

INTRODUCTION

Understanding how cancer cells spread from the primary tumor is important for improving diagnostic, prognostic, and therapeutic approaches that allow control of cancer metastasis. Many of the formative steps that determine the invasive and metastatic potential of carcinoma cells occur within the primary tumor. Much evidence suggests that the progress of cells from normal to invasive and then to metastatic involves progressive transformation through multiple genetic alterations selected by the tumor microenvironment (1). To identify the steps in progression and the genes involved in metastasis, recent emphasis has been on the use of molecular arrays to identify expression signatures in whole tumors with differing metastatic potential (2). A well-recognized problem here is that primary tumors show extensive variation in properties with different regions of the tumor having different growth, histology, and metastatic potential and where only a small subset of cells within the parental tumor population may be capable of metastasizing (3). The array data derived from whole tumors results inevitably in averaging of the expression of different cell types from all of these diverse regions. The expression signature of invasive tumor cells, arguably the population essential for metastasis, may be masked or even lost because of the contribution of surrounding cells, which represent the bulk of the tumor mass. Even so, recent studies of expression profiling of primary tumors suggest that the metastatic potential of tumors is encoded in the bulk of a primary tumor, thus challenging the notion that metastases arise from rare cells within a primary tumor acquired late during tumor progression (4).

This leaves us with a conundrum concerning the contribution of rare cells to the metastatic phenotype. The relative contribution of subpopulations of cells to the invasive and metastatic phenotype of primary tumors has not been assessed due to the difficulty in isolating phenotypically distinct cell populations from whole tumors. In addition, the metastatic cascade has been studied most heavily at the level of extravasation and beyond using experimental metastasis models removing the primary tumor from scrutiny (5). Thus, the microenvironment of the primary tumor that contributes to invasion and intravasation and the process of selection of metastatic cells has not been studied directly.

In this context it has become important to develop technologies to separate pure populations of invasive cancer cells for gene expression studies. To this end, the development of laser capture microdissection has been an important advance (6). However, the identification of cells within the tumor relies on morphology within fixed tissue making uncertain the identity of the collected cells and their behavior within the tumor before fixation. Alternative approaches involve the collection of cells from metastatic tumors and their expansion in culture (7–9). The pitfall of these approaches is that during culturing, the gene expression patterns may change to represent the *in vitro* culture conditions, which are likely to be irrelevant to invasion *in vivo*.

Another approach in determining the cellular mechanisms that contribute to invasion is to collect live cells from the primary tumor based on their ability to invade and profile their gene expression patterns. One of the properties correlated with metastasis is chemotaxis to blood vessels (10). This cell behavior allows cells to orient and move toward blood vessels facilitating their intravasation. On the basis of these observations, we have developed an *in vivo* invasion assay capable of collecting live invasive cells from live primary tumors in intact animals using chemotaxis to growth factors (11). We have used the *in vivo* invasion assay to test the hypothesis that chemotaxis to blood vessels is an important form of egress of carcinoma cells from the primary tumor. Cells have been collected from live rats with tumors of different metastatic potential (11) and from live mice with mammary tumors derived from the expression of the *PyMT* oncogene (12–14).

To perform gene expression profiling using high density arrays on the few hundred cells commonly collected in the *in vivo* invasion assay, it is necessary to amplify mRNA by ~1,000-fold to the amounts required for arrays. It is also necessary to have a pure cell population. Both of these conditions have been met using methods developed recently (14). RNA obtained from as few as 400 cells collected in a single microneedle from the primary tumor, when amplified as cDNA using the PCR-based cDNA amplification technique (15), can be used for microarray expression analysis. This amplification method was validated and demonstrated to retain the original mRNA copy abundance and complexity in the amplified product (14).

In the current study, the collection of invasive cells from the primary tumor using chemotaxis to epidermal growth factor (EGF) in

Received 3/30/04; revised 9/3/04; accepted 9/24/04.

Grant support: NIH [GM25813, CA100324 (J. S. Condeelis), and CA0893208 (R. H. Singer)]. E. Sahai is funded by a Unio Internationale Contra Cancrum Aventis Translational Cancer Research Fellowship.

The costs of publication of this article were defrayed in part by the payment of page charges. This article must therefore be hereby marked *advertisement* in accordance with 18 U.S.C. Section 1734 solely to indicate this fact.

Note: Supplementary data for this article can be found at Cancer Research Online (http://cancerres.aacrjournals.org).

Requests for reprints: Weigang Wang, Department of Anatomy and Structural Biology, Albert Einstein College of Medicine, 1300 Morris Park Avenue, Bronx, NY 10461. Phone: 718-430-4461; Fax: 718-430-8996; E-mail: wgwang@aecom.yu.edu.

the *in vivo* invasion assay was combined with gene expression profiling using these amplification techniques. This technology has allowed the characterization of gene expression patterns of invasive carcinoma cells from the primary tumor without potential artifacts, which arise from the culturing of small populations of cells. We identified a group of genes that define motility pathways that are coordinately up-regulated in invasive cells. These pathways may account for the enhanced migratory behavior of the collected cells. Furthermore, we tested the contribution of these pathways to invasion and metastasis by altering the expression of a master gene that regulates the expression of the common molecule on which these pathways converge.

MATERIALS AND METHODS

***In vivo* Invasion Assay and Fluorescence-Activated Cell Sorting of Primary Tumor Cells.** We used *MTLn3*-derived mammary tumors in rats (16) and the *in vivo* invasion assay described previously (11, 14) to study the gene expression pattern of invasive subpopulations of carcinoma cells within live primary tumors. Briefly, the *in vivo* invasion assay uses microneedles filled with Matrigel and growth factors to collect the invasive cells from primary tumors. Microneedles are held in a clamping device and positioned in the primary tumor with a micromanipulator. Cell collection takes from 1 to 4 hours and was imaged using a multiphoton microscope as described previously (17) by inserting the bevel of a Matrigel and EGF-containing needle into the field of view. A 50-μm z-series consisting of 5-μm steps allows for the imaging of a large number of cells around the needle. One tenth of the volume from each needle was used to determine the number of cells collected. Collected cells were a mixture of carcinoma cells (75%) and macrophages (25%). From the remaining 9/10 volume from the microneedle, macrophages were removed by magnetic separation, and RNA was extracted from purified carcinoma cells as described before (14). To isolate the general population of carcinoma cells from primary tumor, a small piece of tumor was separated from the whole tumor, minced, and filtered twice through a nylon filter to obtain a single cell suspension. Fluorescence-activated cell sorting was performed on the resulting single cell suspensions based on their green fluorescent protein (GFP) expression in tumor cells. GFP-positive tumor cells were collected into a tube and lysed directly for RNA extraction. All of the procedures were done on ice or 4°C.

Because EGF and Matrigel are present in the needle, as a control experiment, we identified genes of which the expression is altered by EGF or Matrigel application. Carcinoma cells from the primary tumor were fluorescence-activated cell sorted as described above. The resulting cells were split and plated on Mattek dishes covered with Matrigel (1:5) in the presence or absence of EGF (1 nmol/L) for 4 hours at 37°C. The cells were then lysed directly on the dish for total RNA extraction.

RNA Amplification, Probe Labeling, and Microarray Hybridization. Common reference RNA standard was prepared by mixing RNA (Ambion, Austin, TX) from rat liver, spleen, brain, and kidney at a 4:2:1:1 RNA weight ratio, respectively. Reference RNA was used to generate probes as a control channel in all of our microarray experiments, which allowed us to use one of the channels as a hybridization control for all of the spots on the microarray. The use of common reference RNA from the same species as the MTLn3 cells allowed the same interspecies cross-hybridization as the background, allowing us to use mouse cDNA microarray for our experiments. The common reference RNA covers a very broad range of gene expression, provides a standard for reducing variation in microarray experiments, and allows for more reliable comparison of gene expression data within and between experiments (18, 19). Mouse cDNA microarrays were obtained from the Albert Einstein College of Medicine cDNA microarray facility (general information about the array printing, quality control, and gene annotation listing are available online[1]). Each slide contained an unbiased, random collection of 27,396 mouse cDNA probe elements (500–1500 bp each) from sequence-verified clone sets by Incyte Genomics (Palo Alto, CA), National Cancer Institute, and Integrated Molecular Analysis of Genomes and their Expression Consortium. Among the 27,396 genes, 47% of genes were annotated known genes.

Microarray analysis was performed in at least three independent repeats, as described previously with minor modification (14). In brief, the RNA from needle collection or fluorescence-activated cell sorting was then concentrated by EtOH precipitation and redissolved in 3.5 μL diethyl pyrocarbonate water. The total RNA was reverse-transcribed directly using the SMART PCR cDNA synthesis kit (Clontech, Palo Alto, CA) according to the manufacturer's protocol. After amplification, cDNAs were purified using the QIAquick PCR Purification kit (Qiagen, Chatsworth, CA) and eluted with 10 mM Tris (pH 8)-1 mM EDTA buffer. Common reference RNA was also amplified using SMART protocol and purified for all of the array hybridizations. Labeling was performed using Label IT (Mirus) following the manufacturer's instructions. Briefly, labeling reactions were prepared by mixing 10X Mirus Labeling Buffer A (10 μL), purified cDNA (3.5 μg), Cy5 (for experimental sample) and Cy3 (for common reference control channel) dye (5 μL) in a total volume of 100 μL. After incubating the reaction mix at 37°C for 1 hour, the two resulting probes were purified by passing through SigmaSpin columns followed by Qiaquick columns. The purified Cy-3 and Cy-5 DNA probes were then combined and concentrated using micron YM 50 columns. Details of slide hybridization, washing, and image collection were described in previous studies (14, 17).

Quality Control, Normalization, and Statistical Analysis of Microarray Data. The scanned images were analyzed using the software Genepix (Axon Instruments, Inc., Foster City, CA), and an absolute intensity value was obtained for each of the channels for the reference RNA and the RNA derived from the cells. The entire raw data set consisting of 27,000 data points was filtered to accommodate a requirement of at least two good quality measurements for each triplicate experiment. Values from only the good quality measurements (where the signal strength was more than twice the SD of the background plus the background) were considered for additional analysis. This quality control filtration resulted in removal of 5,000 spots resulting in 22,000 good spots. Two types of normalization were performed routinely in tandem on all of the experiments using the GeneSpring software package (Silicon Genetics, Redwood City, CA). First, intensity-based normalization was performed, which takes into consideration the overall signal strength of both channels and normalizes the signal strength between all of the different chips, reducing the chance of chip-to-chip variability due to the experiment being performed on different days. Second, a reference channel-based normalization was performed, which takes into consideration the reference channel (which in this case is pooled reference RNA) and normalizes the values in all of the spots. This reduces the chance of spot-to-spot variability. The final data were a result of both these types of normalization.

To determine the signal-to-noise level for up-regulated and down-regulated genes, we calculated the SD of the reference channel in all of the chips and found it to be 0.18 and used five times SD as the cutoff, indicating a high level of fidelity in our data above 2-fold (*i.e.,* 5×0.18). In the genes where a single replicate was flagged and the other two were good, the flagged value was removed and replaced with an average of the other two good values (20). Statistical analysis was performed using Student's *t* test on each of the data sets for each gene. A *P* value was generated for all of the data sets ($n = 3$ for general population and $n = 6$ for invasive cells). Genes that were up- or down-regulated in the arrays performed on control samples (fluorescence-activated cell sorted cells, which were treated with Matrigel and EGF) were removed from the final list of genes specific to the invasive subpopulation of tumor cells.

Real-Time PCR Confirmation. To verify the data obtained from microarrays, quantitative reverse-transcription-PCR (RT-PCR) analysis of selected overexpressed and underexpressed genes was performed by using the iCycler Apparatus (Bio-Rad, Hercules, CA) with sequence-specific primer pairs for all of the genes tested (see Supplementary Table 1 for primer sequences, amplicon size, and melting temperature) as described previously (17). The SYBR Green PCR Core Reagents system (Applied Biosystems, Foster City, CA) was used for real-time monitoring of amplification.

Plasmid Construction, Cell Culture, Transfection, Infection, and Generation of ZBP1 Stable Expression Cell Lines. FLAG-ZBP1 (21) was digested with *Bam*HI/*Xba*I and inserted into the *Bam*HI/*Xba*I sites of EGFP-C1 (Clontech). The EGFP-FLAG-ZBP1, which encodes a fusion protein, was then isolated as Eco47III/*Xba*I restriction fragment, blunt ended, and inserted into a

[1] Internet address: http://www.aecom.yu.edu/home/molgen/facilities.html.

filled *Xho*I site of pMCSVneo (Clontech). This vector contains a viral packaging signal, neomycin resistance gene, and the 5′ and 3′ long terminal repeats from the murine porcine cytomegalovirus. As a result, the long terminal repeat drives high-level constitutive expression of EGFP-FLAG-ZBP1 gene. PHOENIX cells were cultured under standard conditions (22) and were transfected with EGFP-FLAG-ZBP1 using FUGENE (Roche, Indianapolis, IN). Retroviral supernatant was harvested and used to infect MTLn3 cells as described previously (22). Stable MTLn3 cells were selected in the presence of neomycin.

β-Actin Fluorescence *In situ* Hybridization. MTLn3-GFP and MTLn3-ZBP1 cells were grown in α-modified Eagle's medium containing 5% fetal bovine serum and antibiotics (penicillin and streptomycin). Stable MTLn3-ZBP1 cell lines were cultured in the same medium with neomycin to maintain selection of the clones. Cells were grown to 60% to 70% confluency on acid-washed coverslips, washed with PBS, fixed with 4% paraformaldehyde in PBS/5 mmol/L $MgCl_2$, and stored in 70% EtOH at 4°C. *In situ* hybridization for β-actin mRNA was performed as described previously (23). Briefly, the cells were rehydrated in PBS/5 mmol/L $MgCl_2$, permeabilized with 0.5% Triton X-100, incubated with Cy3-labeled probes specific for rat β-actin mRNA, washed, and mounted in Prolong Antifade medium (Molecular Probes, Portland, OR).

Quantitation of β-Actin mRNA Localization. The cytoplasmic distribution of β-actin mRNA within cells was determined using fluorescence *in situ* hybridization and analyzed using two different methods. The first method scored cells as being localized or nonlocalized based on a visual inspection of the pattern of message distribution. Cells containing only perinuclear pools of mRNA were scored as nonlocalizing cells. Cells having message at the periphery or showing a nonperinuclear distribution were scored as localizing cells. The second method plots the fluorescence intensity of the Cy3-labeled β-actin probes as a function of distance from the nucleus. Cell and nuclear edges were traced, and the longest cytoplasmic distance from the nucleus to the edge of the cell was calculated in pixels so that the farthest edge of the cell has a value of 100, and 0 corresponds with the edge of the nucleus. All of the distances within the cell are reported as relative to the longest distance from the nucleus. The fluorescence intensity is reported as a percentage of the total fluorescence intensity of the region analyzed. The ratio of fluorescence intensity distribution plots of MTLn3-ZBP1 normalized to control MTLn3 cells shows the differences in the β-actin mRNA distribution between the two groups.

Cell Morphology. Round cells were defined as having a length to width ratio (in pixels) of between 1 and 1.5. Cells with the ratio >1.5 were scored as polarized. Statistical significance was determined using an unpaired Student's *t* test.

Microchemotaxis Chamber Assay. A 48-well microchemotaxis chamber (Neuroprobe, Cabin John, MD) was used to study the chemotactic response to EGF, following the manufacturer's instructions and as described previously (24).

Blood Burden, Single Cells in the Lung, and Metastases. MTLn3-ZBP1 or MTLn3-GFP cells were injected into the mammary fat pads of female Fisher 344 rats. Tumor cell blood burden was determined as described in a previous study (10). After blood removal and euthanization of the rat, the lungs were removed, and the visible metastatic tumors near the surface of the lungs were counted. For measurement of metastases, excised lungs were placed in 3.7% formaldehyde, mounted in paraffin, sectioned, and stained with H&E. Slices were viewed using a ×20 objective, and all of the metastases in a section containing >5 cells were counted (10).

RESULTS

Gene Expression Patterns Unique to Invasive Tumor Cells. GFP-labeled tumor cells were injected into rat mammary fat pads, and primary tumors were allowed to grow for 2 to 2.5 weeks. To provide insight into the pattern of gene expression associated with chemotactic and invasive carcinoma cells *in vivo*, we compared the gene expression profile of the subpopulation of invasive tumor cells collected from the primary tumor using the *in vivo* invasion assay with that of the general population of GFP-expressing tumor cells sorted from the whole primary tumor by fluorescence-activated cell sorting (Fig. 1*B*). Hereafter, the former population of cells will be called the invasive cells and the latter the general population. The invasive subpopulation of tumor cells was collected into microneedles filled with EGF and Matrigel that were held in the primary tumor for up to 4 hours as described previously (11, 14). Overexpression of the EGF receptor and other family members is correlated with poor prognosis (25). Natural gradients of EGF receptor ligands could be generated by diffusion from the blood as well as stromal cells in the tumor microenvironment (26, 27). Therefore, we used gradients of EGF in the *in vivo* invasion assay to collect invasive carcinoma cells as a physiologically relevant stimulus to mimic tumor cell chemotaxis and invasion to blood vessels observed *in vivo* (28). The collection of the invasive cells was monitored by imaging the GFP-expressing cells with a multiphoton microscope as they migrated to the EGF containing microneedles (Fig. 1*A*). This allowed direct confirmation that collection was due to cell migration and not a passive process.

The collected cells were a mixture of carcinoma cells (75%) and macrophages (25%) as shown previously (14). Macrophages were removed by binding to magnetic beads conjugated with anti-MAC-1, giving a >96% pure population of carcinoma cells for analysis (14). The general population of primary tumor cells was collected by fluorescence-activated cell sorting and plated either on Matrigel or Matrigel and EGF for 4 hours, the interval of time required for microneedle collection, to mimic the collection conditions before purification of the RNA. These controls were done to subtract patterns of gene expression resulting from stimulating cells with Matrigel and EGF and allowed identification of the gene expression pattern unique to the invasive cells (Fig. 1*B*). The genes that were subtracted as part of this control are shown in Supplementary Table 2.

Stringent quality control and statistical analysis were performed on the datasets collected from the invasive and general population. Firstly, data were only considered from those spots that had a significantly higher signal value than the background as defined in Materials and Methods. Those genes that did not meet these criteria in more than one spot out of three were removed from the dataset. Student's *t* test was performed on the data sets to determine the level of significance between the two datasets (Tables 1 and 2).

Differential gene expression analysis comparing the invasive and general populations of tumor cells revealed 1,366 genes of known functions that were differentially expressed by ≥2-fold compared with 27,000 arrayed (Supplementary Table 3). As shown in Fig. 1*C,* genes with known functions were divided into 10 different functional categories based on definitions provided by the gene-ontology consortium (29).[2] Briefly each of the annotated genes was put into the functional category that best describes its function. To determine the significance of changes in gene expression in each of the functional categories of the genes represented in our arrays, the number of genes regulated either up or down in the invasive cells for each functional category was compared with all of the genes on the array and the statistical significance calculated using significance analysis of microarrays, software that performs significance analysis to determine changes between the samples and replicates (20). We also used χ^2 analysis to calculate the random occurrence of genes in any one of the functional categories (A detailed table indicating each of the functional categories and the number of genes in each of them that are either up or down-regulated is given in Supplementary Table 4*A*). The average *P* value for all of the 1,366 genes was 0.0136. Given a *P* value like this, ~367 genes would have been up- or down-regulated randomly on a 27,000 gene array at the 2-fold cutoff used. The probability that this pattern shown in Fig. 1*C, panel c* is generated randomly is very low, because the numbers of genes in each functional category

[2] Internet address: http://www.geneontology.org.

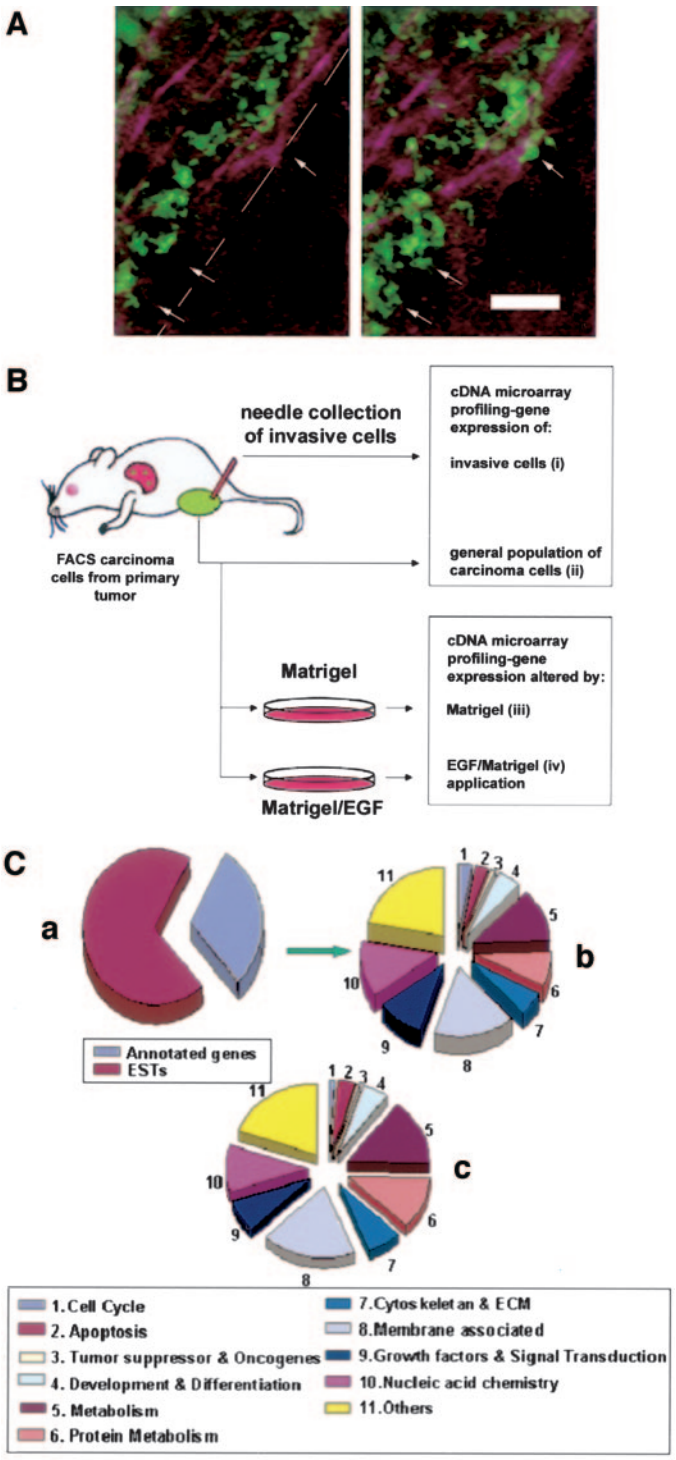

Fig. 1. *In vivo* selection and gene expression analysis of the highly invasive subpopulation of breast cancer cells collected by chemotaxis. *A,* multiphoton images of live cell collection in a MTLn3-derived tumor. GFP-expressing carcinoma cells (*green*) are seen moving toward the bevel (*dashed line* delineates edge) of a microneedle filled with Matrigel and 25 nmol/L EGF. *Purple lines* are extracellular matrix of the primary tumor imaged due to its second harmonic signal. *Arrows* indicate the final location of invading cells in both frames over the time lapse interval of 1 hour. *Scale bar* = 25 μm. *B,* schematic representation of the chemotaxis-based selection process. MTLn3-derived mammary tumors in rats and the *in vivo* invasion assay were used to study the gene expression pattern of the invasive subpopulation of carcinoma cells within live primary tumors. Invasive cells were collected using the *in vivo* invasion assay (needle collection). FACS based on GFP expression in tumor cells was performed to isolate the general population of carcinoma cells from the primary tumor. RNA extraction, probe labeling, and microarray analysis were carried out. Carcinoma cells from primary tumor were fluorescence-activated cell sorted as described above. The resulting cells were split and plated on a Mettek dish covered with Matrigel (1:5) in the presence (*iv*) or absence of 1 nmol/L EGF (*iii*) for 4 hours at 37°C. The cells were then lysed directly on the dish for total RNA extraction, probe labeling, and microarray analysis. Genes that were up or down-regulated on control experiments (comparison: *iii versus ii* and *iv versus ii*) were removed from the list of differentially expressed genes obtained when comparing *i* and *ii*. The resulting final list of 1,366 genes is shown in Supplementary Table 3. *C,* summary diagram showing functional categories of the genes regulated in the invasive cells. These pie charts represent the relative proportion of genes in 10 categories based on their function using Gene-ontology Consortium classifications. *Pie a* represents the relative proportion of annotated spots compared with expressed sequence tags on the array. *Pie b* shows the proportional representation of the functional groups into which the genes annotated in a fall. *Pie c* shows the proportional representation of the functional groups into which the genes regulated in the invasive cells fall. (FACS, fluorescence-activated cell sorting)

shown in Fig. 1*C, panels b* and *c* (Supplementary Table 4*A*), is not equal.

Of these categories we have studied three in more detail. The genes of which the expression is regulated up or down in the functional category called cell cycle (Fig. 1*C, panel c,* #1) in the invasive cells compared with the general population was informative. In particular, genes that enhance cell proliferation were down, and those that repress proliferation were up (Supplementary Table 4*B*) indicating that the cell proliferation activity of invasive cells is repressed (30). Second, the number of genes regulated in the category called apoptosis (Fig. 1*C, panel c,* #2) is significantly higher in invasive cells collected into needles compared with the general population of tumor cells collected by fluorescence-activated cell sorting from the whole primary tumor. In particular, antiapoptotic genes are up, and proapoptotic genes are down-regulated indicating a survival advantage for invasive cells (31). Third, of particular relevance to the migratory behavior of invasive cells, there is an increase in the number of regulated genes in the cytoskeleton and extracellular matrix (Fig. 1C-c, #7; Table 1). In particular, the genes coding for the minimum motility machine, *i.e.,* the cofilin, capping protein and Arp2/3 pathways, that regulate β-actin polymerization, and therefore the motility of carcinoma cells, were dramatically up-regulated (Fig. 2). These pathways may account for the enhanced migratory behavior of the collected cells. Changes in these three categories of gene expression indicate that invasive cells are neither dividing nor apoptotic but are intensely migratory.

Gene expression patterns of metastatic cells obtained in a previous study comparing metastatic and nonmetastatic cell lines and tumors derived from them (17), were compared with differences in the patterns of gene expression between invasive and noninvasive tumor cells of the primary tumor observed in this study. From these comparisons a set of common genes emerged that were changed in all of the cases (Table 2). This pattern of genes represents a potential invasion signature that may be common to all of the cells in the primary tumor of heightened metastatic potential. This study demonstrates the value of comparing cell lines and tumors of different metastatic potential with invasive cells collected from primary tumors.

Genes Involved in Invasion. To be collected in the *in vivo* invasion assay, carcinoma cells must be capable of moving toward and crawling into the extracellular matrix of the microneedle within the 4-hour collection interval. If a cell moves 2 cell diameters during this interval to gain entry to the microneedle it would have a minimum speed of 0.2 μm/min, similar to the velocity of carcinoma cells *in vitro*. However, carcinoma cells move in the primary tumor at speeds up to 10 times this minimum value (28) indicating that cells from hundreds of microns away from the microneedle can be recruited for collection and that the cells may penetrate the extracellular matrix in the collecting microneedle. Consistent with this prediction is the observation that carcinoma cells are found deep within the matrix of the collecting microneedle indicating that cells have traveled hundreds of microns during the collection interval indicating speeds much greater than 0.2 μm/min *in vivo*.

As shown in Table 1, based on the microarray analysis, many genes

Table 1 List of motility-related genes differentially expressed in the invasive subpopulation of tumor cells

Acc no.	Gene description	Invasive cells/general population	*P* value
AA414612	Capping protein α1*	4.00	0.008
AW556230	Cell division cycle 42*	3.96	0.007
AU015486	Capping Protein α2	3.89	0.016
C79581	Moesin*	3.67	0.020
C86972	Arp 2/3 complex subunit p16*	3.52	0.011
AW538432	Rho interactin protein 3*	3.33	0.005
AU015879	LIM-kinase 1*	3.24	0.006
AA285584	Palladin	3.12	0.003
AW555565	Zyxin	2.93	0.014
W10023	Catenin β	2.88	0.029
C76867	Tropomyosin α chain	2.86	0.001
AU023806	Rho-associated coiled-coil forming kinase 1*	2.71	0.002
AW536576	Testis expressed gene 9	2.67	0.006
AI324089	Phosphatidylinositol-4-phosphate 5-kinase type II α*	2.60	0.005
AI427644	Epidermal growth factor receptor*	2.59	0.019
AW541453	Capping protein (actin filament), gelsolin-like	2.53	0.020
C86107	Actinin α3*	2.52	0.003
AW543636	Annexin A5	2.47	0.013
AA052404	CRIPT protein	2.32	0.011
AA014771	Protein kinase C, ζ*	2.30	0.011
AW546733	Arp 2/3 complex subunit p21*	2.22	0.014
AA538228	RAB25, member RAS oncogene family	2.19	0.035
AA275245	Vinculin	2.16	0.021
AA386680	Kinesin family member 5B	2.13	0.015
AW536843	Chaperonin subunit 4 (δ)	2.06	0.009
AW536183	Chaperonin subunit 3 (γ)	2.06	0.042
AI326287	Tubulin α-4 chain	2.05	0.046
AW553280	Integrin β1 (fibronectin receptor β)	2.00	0.013
AW536098	Cofilin 1, nonmuscle*	2.00	0.023
AU017992	Kinectin 1	2.00	0.005
AW557123	Downstream of tyrosine kinase 1	2.00	0.013
AW549817	Burkitt lymphoma receptor 1	2.00	0.021
AA272097	Fibroblast growth factor receptor 1	0.54	0.004
AA073514	Zip code binding protein 1*	0.11	0.004

NOTE. Genes associated with motility are displayed in this table, and the ratios on the right indicate the level of expression in the invasive compared to the general population of cells of the primary tumor. *P* values indicate the result of Student's *t* test performed on these genes.

*These results have been validated by quantitative real-time–PCR.

associated with motility are up-regulated in the invasive cells compared with the general population of cells. To make sense of Table 1 it is necessary to consider that the motility cycle of chemotactic carcinoma cells is composed of five steps: signal sensing, protrusion toward the signal source, adhesion, contraction, and tail retraction (32). Of particular relevance to chemotaxis and invasion, the protrusion of a pseudopod toward the chemotactic signal initiating the motility cycle is the key step in defining the leading edge of the cell and, therefore, its direction during migration (32). Protrusion is driven by actin polymerization-based pushing against the cell membrane, and this requires the minimum motility machine composed of cofilin, Arp2/3 complex, and capping protein acting on their common downstream effector, β-actin (33). The elevated expression of any one of these three effectors is expected to significantly enhance the speed of migration of cells, because doubling the amount of Arp2/3 complex, capping protein, or cofilin in the reconstituted minimum motility machine can increase protrusion rate by 10 times (34). Therefore, it is significant, as shown in Fig. 2*A,* that the genes coding for all three of the end-stage effectors, the Arp2/3 complex (the p16 and p21 subunits), capping protein, and cofilin, are up-regulated by at least 2-fold each. Furthermore, the genes coding for the pathways regulating the activities of Arp2/3 complex (WAVE3), capping protein, and cofilin are coordinately up-regulated in the invasive cell population.

We verified, using real-time PCR, the array results for genes detected to have changed expression in these pathways. As shown in Fig. 2*B,* the same pattern of expression was observed in the invasive cells with both microarray and real-time PCR analysis.

In the cofilin pathway, genes for *ROCK1* and *LIMK 1* representing the inhibitory branch of the cofilin pathway are up-regulated. In addition, *cofilin* and *PKCz*, representing the stimulatory side of the cofilin pathway, are up-regulated. LIM kinase is activated by ROCK, which is regulated by Rho-GTP. ROCK (35) can phosphorylate LIM kinase thereby activating it to phosphorylate cofilin, which inhibits cofilin. Inhibition of LIM kinase activity involves its phosphorylation by the unconventional PKCz (36).

Similar increases in both the stimulatory and inhibitory parts of the capping protein pathway are up-regulated in invasive carcinoma cells (Fig. 2*A*). The expression of both the α and β subunits of capping protein is increased. In addition, genes that antagonize capping protein function such as the type II α isoform of PI4, 5 kinase, and Mena are up-regulated (37, 38).

ZBP1 as a Master Gene Regulating Invasion and Metastasis. A gene that is strongly down-regulated in invasive cells is Zip-code binding protein (ZBP1; Tables 1 and 2; Fig. 2). ZBP1 is a 68-kDa RNA-binding protein that binds to the mRNA zipcode of β-actin mRNA and functions to localize the mRNA to the leading edge of crawling cells. β-Actin is the preferred isoform of actin for the polymerization of filaments at the leading edge of cells and, therefore, is acted on by the cofilin, capping protein, and Arp2/3 pathways (39). ZBP1 may determine the sites in cells where the Arp2/3 complex, capping protein, and cofilin pathways converge by controlling the sites of targeting of β-actin mRNA and the location of β-actin protein that is the common downstream effector of these pathways (Fig. 2*A*). β-Actin mRNA localization is required for the generation of intrinsic and stable cell polarity that is characteristic of normal primary fibroblasts and epithelial cells. Disruption of ZBP1-mediated β-actin mRNA targeting leads to cells without intrinsic cell polarity, *i.e.,* cells that are more amoeboid (39). Loss of β-actin mRNA targeting is correlated with the loss of intrinsic stable cell polarity, increased amoeboid movement in metastatic carcinoma cell lines *in vitro* and *in vivo* (17, 23), and increased chemotaxis. Therefore, ZBP1 expression might suppress the chemotactic and invasive potential of carcinoma

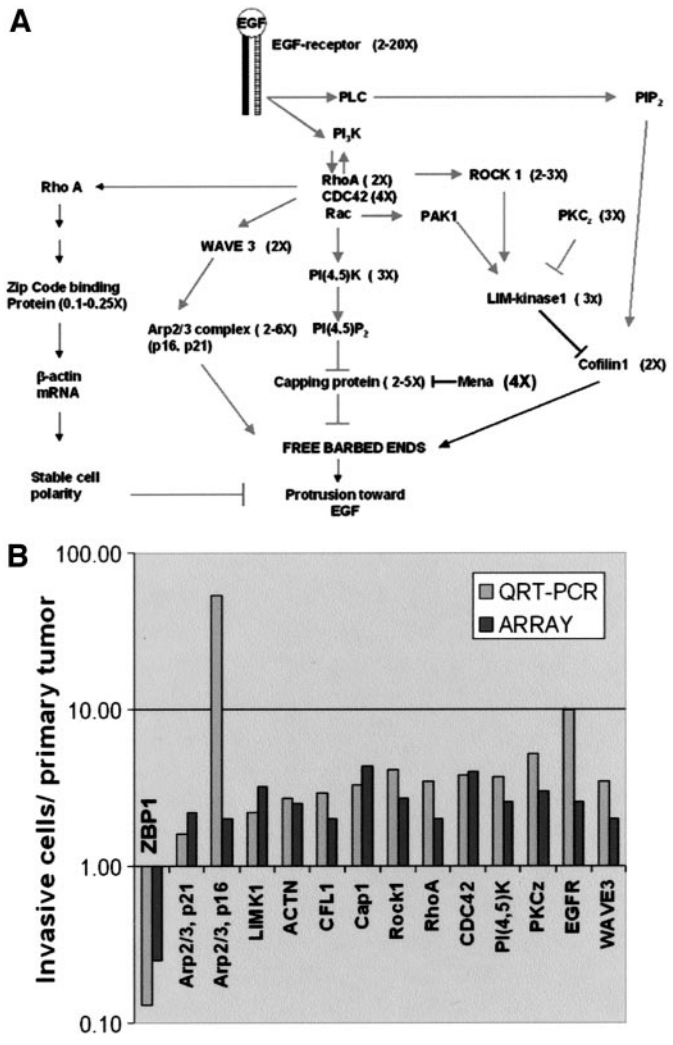

Fig. 2. Motility genes differentially expressed in invasive cells. *A.* The minimum motility machine pathways in the invasive cells are up-regulated. Pathways leading to the generation of protrusive force in response to EGF are shown. The extent of up-regulated expression of differentially expressed genes is indicated next to each component of the pathway as *nX*. The expression level of Mena shown here was calculated by quantitative RT-PCR as 6.0±1.1. *B,* validation of microarray results for selected genes by QRT-PCR. Expression analyses of invasive cells compared with the general population of cells in the tumor by QRT-PCR gives the same pattern as did cDNA microarrays. (QRT-PCR, quantitative real time PCR; CFL, cofilin; cap1, capping protein)

cells in tumors, which is proposed to require amoeboid movement and chemotaxis.

To test the hypothesis that ZBP1 expression can suppress the chemotaxis and invasion of cells *in vivo*, the full-length ZBP1 gene was subcloned in a pMCSVneo vector (Fig. 3*A*) and transfected into the parental MTLn3 cells. Data from Western blot analysis (Fig. 3*B*) confirmed that stable clones transfected with pEGFP-FLAG-ZBP1 express higher levels of ZBP1 compared with untransfected cells. To account for any effects that might arise from the introduction of EGFP into cells, MTLn3 cells transfected with pGreenLantern-1 vector (Life Technologies, Inc., Gaithersburg, MD) were used as control.

To investigate the effects of expressing ZBP1 in carcinoma cells on β-actin mRNA targeting, the ZBP1-expressing cells were analyzed using fluorescence *in situ* hybridization. As shown in Fig. 4*A—D,* the expression of ZBP1 in carcinoma cells rescued the targeting of β-actin mRNA asymmetrically to a cell edge. Furthermore, cells expressing ZBP1 became polarized (Fig. 4*E*).

To investigate the chemotactic properties of the ZBP1-expressing cells, two independent clones of ZBP1-expressing cell lines were characterized. Chemotaxis was measured in a Boyden chamber. ZBP-1-expressing cells migrated through the filter in response to EGF poorly compared with the parental MTLn3 cells (Fig. 5*A*), indicating that chemotaxis was inhibited. This was true for both ZBP1 clones. Furthermore, the ability of carcinoma cells to invade microneedles in the *in vivo* invasion assay was greatly reduced for tumors derived from MTLn3 cells expressing ZBP1 (Fig. 5*B*) indicating a reduction in chemotaxis and invasion *in vivo*.

Injection of the ZBP1-expressing cells into the mammary fat pads of rats resulted in tumors that were less metastatic. The metastatic potential of these tumors was characterized as the efficiency of intravasation, by measuring the number of tumor cells present in circulating blood (Fig. 5*C*) and the number of spontaneously occurring lung metastatic tumors (Fig. 5*D*). However, as shown in Fig. 5*E,* tumor growth was not significantly affected by increasing the expression of ZBP1.

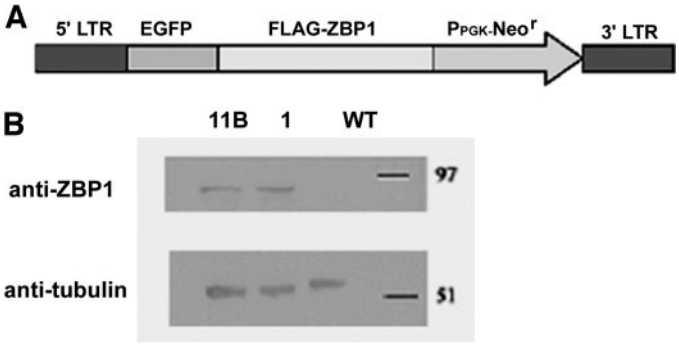

Fig. 3. ZBP1 construct and its expression in MTLn3 cells. *A.* The full-length ZBP1 gene was subcloned in a pMCSVneo vector and transfected into parental MTLn3 cells. The control plasmid used in the experiments was the pGreenLantern-1. *B.* Stable MTLn3-ZBP1 clones 1 and 11B were selected in the presence of neomycin. The Western blot shows the increased ZBP1 protein expression in these two separate clones.

Table 2 Genes differentially expressed in invasive cells identified in this study showing the same pattern of expression in cell lines and metastatic tumors derived from them

Gene name	Acc no.	Metastatic/nonmetastatic, cell line*	Metastatic/nonmetastatic, tumor†	Needle/FACS‡	*P* value	Gene function
Collagen, type III, α1	W89883	0.01	0.15	0.19	0.001	Extracellular matrix composition
G-protein coupled receptor 26	C77414	0.14	0.2	0.46	0.0002	Signal transduction
Zip code binding protein 1	AA073514	0.08	0.03	0.11	0.004	Cell polarity
Fibroblast growth factor receptor 1	AA272097	0.32	0.35	0.54	0.004	Signal transduction
ARP2/3 Complex 16 kD subunit	C86972	6.31	5.45	3.52	0.011	Minimum motility machine
Tight junction protein 2	AU044024	2.96	2.16	3.4	0.019	Adhesion molecules
RAB25 member Ras oncogene family	AA538228	7.99	6.38	2.18	0.017	Signal transduction
Epidermal growth factor receptor	AI427644	20.12	2.0	2.6	0.019	Signal transduction

NOTE. Top part indicates lower expression and the lower part of the table represents overexpression. *P* values indicate the result of Student's *t* test performed on these genes. Taken together these genes outline a signature of invasion and indicate that a number of interacting pathways are involved in invasion.

Abbreviations: FACS, fluorescence-activated cell sorting.

*Metastatic cell line, MTLn3; nonmetastatic cell line, MTC.

†Tumor derived from injection of MTLn3 or MTC.

‡Needle, cells collected into needle by chemotaxis = invasive; fluorescence-activated cell sorting, cells obtained from whole tumor by FACS = general population.

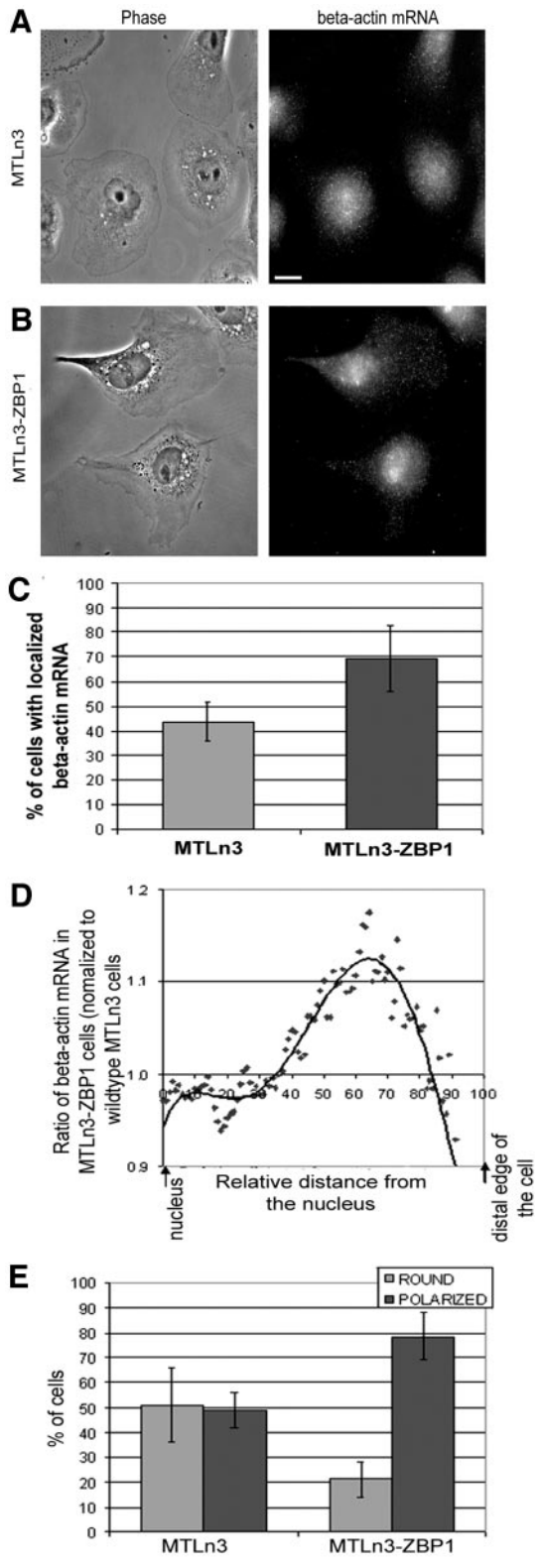

Fig. 4. ZBP1 reexpressing cells localize β-actin mRNA asymmetrically to the cell periphery and are polarized. *In situ* hybridization using cy3-labeled probes against rat β-actin mRNA was used to show the distribution of message within cells grown continuously in serum. Both parental MTLn3 (*A*) and MTLn3-ZBP1 (*B*) cells have perinuclear pools of β-actin mRNA. However, ZBP1 reexpression increases the localization of β-actin mRNA to the cell periphery (*B*). *Scale bar* = 10 μm. *C.* MTLn3-ZBP1 reexpressing cells show a 1.6-fold increase in localized β-actin mRNA to the cell periphery compared with parental cells ($P < 0.01$, Student's *t* test). *Bars,* ±SD. *D.* The localization of β-actin mRNA in parental and ZBP1 reexpressing cells to the cell periphery was quantified by plotting the location of mRNA as a function of distance from the nucleus. MTLn3-ZBP1 reexpressing cells localize β-actin mRNA to more distal regions of the cell than parental cells do. ZBP1 reexpression changes the message distribution along the length of the cell so that the mRNA distribution extends past the perinuclear region almost reaching the far end of the cell (see *B*). *E.* The cell morphology of ZBP1 reexpressing cells is more polarized. MTLn3 cells grown continuously in serum show heterogeneity in cell shape with ~50% of the cells rounded and the other 50% polarized. The percentage of polarized cells in MTLn3-ZBP1 cells increases to 80%, which is a 1.6-fold increase compared with parental MTLn3 cells ($P < 0.01$, Student's *t* test).

DISCUSSION

Patterns of Gene Expression in Invasive Carcinoma Cells. By comparing gene expression patterns of invasive cells to those of the general population of carcinoma cells in the same primary tumor, we were able to find patterns in the regulation of gene expression unique to the invasive subpopulation of cells. Our results indicate that the invasive cells are a population that is neither proliferating nor apoptotic but intensely motile. Whereas increased cell proliferation during tumor development has been associated with poor prognosis in patients (40), the results reported both here and in previous studies (10) indicate that tumor size is neither correlated with invasion nor the ability of cells to metastasize to distant organs. In addition, invasive cells show down-regulation of genes associated with apoptosis and up-regulation of genes for cell survival (31). This is consistent with previous work where it was shown that cell survival genes were up-regulated in metastatic tumors as compared with nonmetastatic tumors (17) and suggests that the invasive subpopulation may contribute to this expression profile in whole metastatic tumors.

In addition, in this study we have identified a pattern of gene expression common to metastatic cell lines and tumors and the invasive population of cells in primary tumors (Table 2). This pattern of genes represents a potential invasion signature that may be common to all cells in the primary tumor of heightened metastatic potential. This suggests that the invasive population of cells has enhanced an expression pattern of a subset of genes that is characteristic of the differences between metastatic and nonmetastatic cell lines and tumors. This is emphasized by the fact that the invasive subpopulation of cells collected using the *in vivo* invasion assay is from tumors derived initially from common genetic background, *i.e.,* a single cell line, the MTLn3. This indicates that as the tumor progresses, highly invasive cells are selected in which a pattern of gene expression present in metastatic cells and tumors is enhanced over the pattern of expression of the cells that remain behind in the primary tumor. This pattern may represent a signature for invasion that may be general to a number of carcinomas.

Recently, several studies of human primary breast tumors have generated gene expression signatures that are predictive of metastasis and poor survival (4, 41). Among the genes identified in our study comparing invasive cells to the general population (Supplementary Table 2), only *SNRPF* (*small nuclear ribonucleoprotein F*) and *LMNB1* encoding Lamin B1 were identified in common out of 8 of the signature genes highly expressed in solid tumors in humans associating with metastasis and poor clinical outcome (4). None of the genes found in common with metastatic cell lines and tumors (Table 2) were represented in the gene expression patterns predicting poor survival in these studies. Additional work with invasive cells collected from a variety of human tumors will be required to evaluate the generality of our invasion signature.

Cell Motility Genes and Their Roles in Cancer Invasion. Chemotaxis and cell migration in response to EGF is correlated with invasion, intravasation, and metastasis in animal models of breast cancer (10, 11, 28). A major result of this study is the finding that genes of the minimum motility machine are up-regulated, predicting that protrusion velocity will be increased. Because the site of protrusion sets cell direction and, therefore, defines chemotaxis, this step in

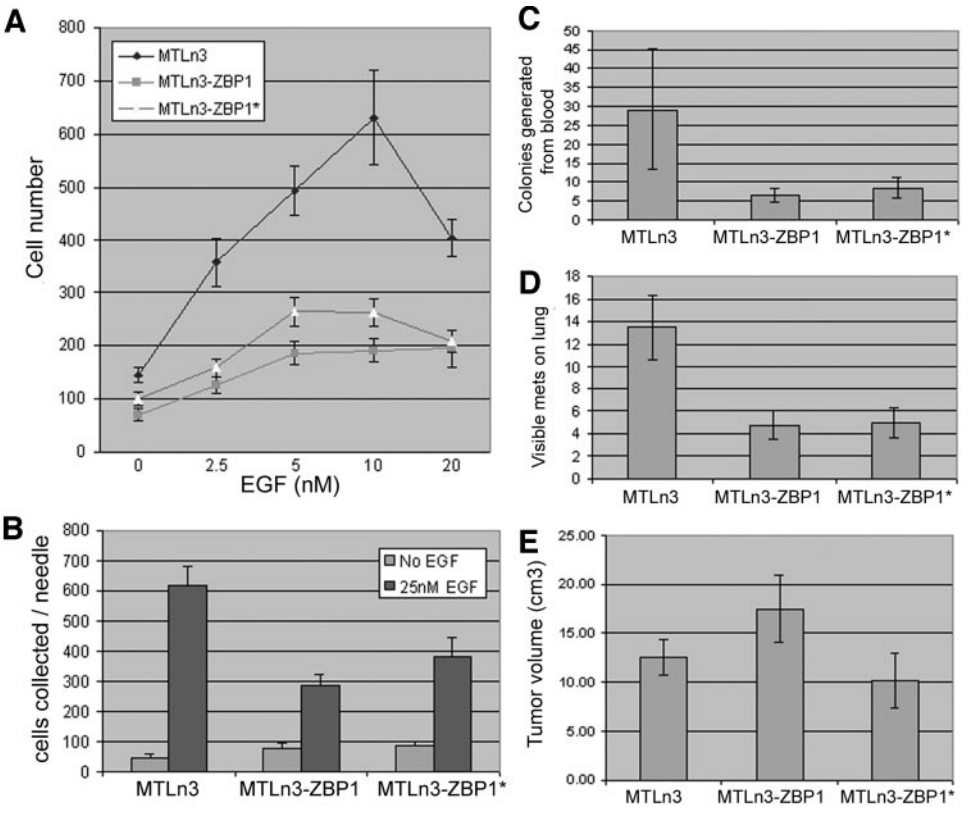

Fig. 5. ZBP1 expression inhibits tumor invasion and metastasis. *A.* ZBP1 expression inhibits cell motility. Chemotaxis was measured in a Boyden chamber. ZBP1-expressing cells migrated through the filter in response to EGF poorly compared with the parental MTLn3 cells *B.* ZBP1 expression inhibits chemotaxis and invasion *in vivo* as confirmed by the *in vivo* invasion assay. The ability of carcinoma cells to invade microneedles placed into primary tumors derived from MTLn3 cells expressing ZBP1 was greatly reduced. Needles that do not contain EGF represent background. *C* and *D.* ZBP1-expressing cells show lower metastatic potential. The number of tumor cells present in circulating blood (*C*) and the number of lung metastatic tumors (*D*) were greatly reduced in animals with tumors prepared with cells expressing ZBP1 ($P < 0.05$, by Mann-Whitney Test). However, as shown in *E,* tumor growth was not affected by increasing the expression of ZBP1; *bars,* ±SD.

the motility cycle may be a key in determining invasive potential. These results are consistent with the 10-fold higher velocity of cell migration toward blood vessels and EGF-filled microneedles, both sources of chemoattractant, observed in primary tumors of live rats and mice compared with the velocity of movement of their cultured cell counterparts (10, 11, 16, 17, 28). Consistent with these results is the finding that inhibition of the nucleation activity of Arp2/3 complex in carcinoma cells in culture inhibits chemotaxis to EGF (42) and that cofilin activity is required for cell motility (43), cell direction (44), and chemotaxis (45) in carcinoma cells.

As seen in Fig. 2*A,* genes coding for key components of the pathways regulating the minimum motility machine are coordinately up-regulated. Both the stimulatory and inhibitory parts of the cofilin and capping protein pathways are up-regulated. This is consistent with the importance of transients of actin polymerization in the chemotaxis of crawling cells (45, 46). If actin polymerization is either sustained or inhibited, cell motility ceases. By up-regulating both the stimulatory and inhibitory parts of pathways leading to actin polymerization, actin polymerization occurs as a transient (47) allowing the cell to adjust and move according to directional signals (45).

In previous studies, LIM kinase 1 was shown to be overexpressed in metastatic breast and prostate tumors (48, 49). Overexpression of LIM kinase 1 in tumor cell lines increased their motility and invasiveness *in vitro* (48) and *in vivo* (49). Reduction in the expression of LIM kinase 1 in metastatic prostate cell lines decreased invasiveness in Matrigel invasion assays (48). These results are consistent with ours shown here that LIM kinase 1 is more highly expressed in the invasive cell population.

However, it has also been reported that increased expression of LIM kinase 1 in carcinoma cells significantly reduces their cell motility, because the phosphorylation of cofilin by LIM kinase 1 abolishes EGF-induced actin nucleation and polymerization (50). Our study may resolve this paradox by demonstrating that in invasive cells collected from primary tumors both the stimulatory and inhibitory pathways to LIM kinase 1 and cofilin are overexpressed together thereby increasing the rate of cofilin activation and inactivation in invasive carcinoma cells resulting in actin polymerization transients and enhanced cell motility as predicted previously (48–51) and observed experimentally (44, 45).

Among the genes up-regulated in the pathways of Fig. 2, several have been implicated in invasion and metastasis in previous studies. Clinical studies of bladder cancer, breast cancer, and colorectal cancer have implicated Rock (52), Mena (53), and the Arp2 and 3 subunits of the Arp2/3 complex (54), respectively, as up-regulated in these cancers.

ZBP1 in Metastasis. ZBP1 is required for the targeting of β-actin mRNA asymmetrically to the cell edge, and this helps to define an intrinsic and stable cell polarity. Cells that lack an intrinsic and stable polarity are more chemotactic to exogenous gradients presumably because there is no intrinsic polarity to be overcome by the exogenous chemotactic signal, and the cell can turn in any direction to respond to the gradient (55, 56). In carcinoma cells, an EGF gradient generates transients of actin polymerization that lead to transient cell polarity toward the source of the gradient (45). Therefore, in tumors, cells that have proceeded through the epithelial mesenchymal transition to the point where all remnants of the intrinsic and stable cell polarity of the original epithelium are lost are predicted be more efficient at responding to external chemotactic signals. This may account for the enhanced ability of carcinoma cells to chemotax to blood vessels and to intravasate in metastatic primary tumors (10, 28).

In the present study, invasive tumor cells isolated from primary mammary tumors using chemotaxis express much lower levels of ZBP1 than cells that remain behind in the primary tumor, although both cell populations were derived from the same progenitor MTLn3 cells (Tables 1 and 2). Furthermore, as shown in the current study, reexpression of ZBP1 rescues both β-actin mRNA targeting and

intrinsic cell polarization. This is correlated with a reduction in chemotaxis, intravasation, and metastasis.

ZBP1 is a member of a family of RNA binding proteins expressed in embryonic and transformed cells. All of these proteins contain four COOH-terminal hnRNP K homology domains and two NH_2-terminal RNA recognition motifs (57). Expression of members of this protein family occurs during development and becomes undetectable after birth but is elevated in a variety of human cancers (57). Consistent with this pattern of expression is our result that nonmetastatic cells and tumors express detectable levels of ZBP1 (17). Overexpression of a mouse homologue of ZBP1 called CRD-BP causes mammary tumors in transgenic mice (58). However, lung metastases were not detected in the CRD-BP-induced tumors. This is consistent with our results reported here that ZBP1 expression suppresses lung metastasis and that invasive and metastatic cells and tumors exhibit low levels of ZBP1 expression compared with nonmetastatic cells and tumors (Table 2). The ability of CRD-BP to induce tumor formation suggests additional roles for this family of RNA binding proteins in tumorigenesis beyond its demonstrated suppression of metastasis. One possible role is the ability of the CRD-BP to stabilize c-myc mRNA in cells in culture (59).

The results reported here indicate that ZBP1 is a "metastasis suppressor" and, together with mRNA targeting status and analysis of tumor cell polarity around blood vessels discussed above, might be used to predict the metastatic potential of mammary tumors.

ACKNOWLEDGMENTS

We thank Dr. Erwin Bottinger and the staff of Albert Einstein Biotechnology Center for their invaluable help and expertise. We are grateful to Aldo Massimi (Albert Einstein College of Medicine Microarray Core) and members of the Analytical Imaging Facility for support and advice. We thank Alex Rodriguez and Shailesh Shenoy for their essential contributions to the fluorescence *in situ* hybridization analysis.

REFERENCES

1. Hanahan D, Weinberg RA. The hallmarks of cancer. Cell 2000;100:57–70.
2. Liotta LA, Kohn EC. The microenvironment of the tumour-host interface. Nature (Lond) 2001;411:375–9.
3. Fidler IJ, Kripke ML. Metastasis results from preexisting variant cells within a malignant tumor. Science (Wash DC) 1977;197:893–5.
4. Ramaswamy S, Ross KN, Lander ES, Golub TR. A molecular signature of metastasis in primary solid tumors. Nat Genet 2003;33:49–54.
5. Chambers AF, Groom AC, MacDonald IC. Dissemination and growth of cancer cells in metastatic sites. Nat Rev Cancer 2002;2:563–72.
6. Bonner RF, Emmert-Buck M, Cole K, et al. Laser capture microdissection: molecular analysis of tissue. Science (Wash DC) 1997;278:1481,1483.
7. Clark EA, Golub TR, Lander ES, Hynes RO. Genomic analysis of metastasis reveals an essential role for RhoC. Nature (Lond) 2000;406:532–5.
8. Kang Y, Siegel PM, Shu W, et al. A multigenic program mediating breast cancer metastasis to bone. Cancer Cell 2003;3:537–49.
9. Ree AH, Engebraaten O, Hovig E, Fodstad O. Differential display analysis of breast carcinoma cells enriched by immunomagnetic target cell selection: gene expression profiles in bone marrow target cells. Int J Cancer 2002;97:28–33.
10. Wyckoff JB, Jones JG, Condeelis JS, Segall JE. A critical step in metastasis: in vivo analysis of intravasation at the primary tumor. Cancer Res 2000;60:2504–11.
11. Wyckoff JB, Segall JE, Condeelis JS. The collection of the motile population of cells from a living tumor. Cancer Res 2000;60:5401–4.
12. Lin EY, Gouon-Evans V, Nguyen AV, Pollard JW. The macrophage growth factor CSF-1 in mammary gland development and tumor progression. J Mammary Gland Biol Neoplasia 2002;7:147–62.
13. Lin EY, Nguyen AV, Russell RG, Pollard JW. Colony-stimulating factor 1 promotes progression of mammary tumors to malignancy. J Exp Med 2001;193:727–40.
14. Wang W, Wyckoff JB, Wang Y, Bottinger EP, Segall JE, Condeelis JS. Gene expression analysis on small numbers of invasive cells collected by chemotaxis from primary mammary tumors of the mouse. BMC Biotechnol 2003;3:13.
15. Zhu YY, Machleder EM, Chenchik A, Li R, Siebert PD. Reverse transcriptase template switching: a SMART approach for full-length cDNA library construction. Biotechniques 2001;30:892–7.
16. Farina KL, Wyckoff JB, Rivera J, et al. Cell motility of tumor cells visualized in living intact primary tumors using green fluorescent protein. Cancer Res 1998;58:2528–32.
17. Wang W, Wyckoff JB, Frohlich VC, et al. Single cell behavior in metastatic primary mammary tumors correlated with gene expression patterns revealed by molecular profiling. Cancer Res 2002;62:6278–88.
18. Goswami S, Sheets NL, Zavadil J, et al. Spectrum and range of oxidative stress responses of human lens epithelial cells to H2O2 insult. Invest Ophthalmol Vis Sci 2003;44:2084–93.
19. Novoradovskaya N, Whitfield ML, Basehore LS, et al. Universal Reference RNA as a standard for microarray experiments. BMC Genomics 2004;5:20.
20. Tusher VG, Tibshirani R, Chu G. Significance analysis of microarrays applied to the ionizing radiation response. Proc Natl Acad Sci USA 2001;98:5116–21.
21. Farina KL, Huttelmaier S, Musunuru K, Darnell R, Singer RH. Two ZBP1 KH domains facilitate beta-actin mRNA localization, granule formation, and cytoskeletal attachment. J Cell Biol 2003;160:77–87.
22. Dal Canto RA, Shaw MK, Nolan GP, Steinman L, Fathman CG. Local delivery of TNF by retrovirus-transduced T lymphocytes exacerbates experimental autoimmune encephalomyelitis. Clin Immunol 1999;90:10–4.
23. Shestakova EA, Wyckoff J, Jones J, Singer RH, Condeelis J. Correlation of beta-actin messenger RNA localization with metastatic potential in rat adenocarcinoma cell lines. Cancer Res 1999;59:1202–5.
24. Segall JE, Tyerech S, Boselli L, et al. EGF stimulates lamellipod extension in metastatic mammary adenocarcinoma cells by an actin-dependent mechanism. Clin Exp Metastasis 1996;14:61–72.
25. Nicholson RI, Gee JM, Harper ME. EGFR and cancer prognosis. Eur J Cancer 2001;37 Suppl 4:S9–15.
26. O'Sullivan C, Lewis CE, Harris AL, McGee JO. Secretion of epidermal growth factor by macrophages associated with breast carcinoma. Lancet 1993;342:148–9.
27. LeBedis C, Chen K, Fallavollita L, Boutros T, Brodt P. Peripheral lymph node stromal cells can promote growth and tumorigenicity of breast carcinoma cells through the release of IGF-I and EGF. Int J Cancer 2002;100:2–8.
28. Condeelis J, Segall JE. Intravital imaging of cell movement in tumours. Nat Rev Cancer 2003;3:921–30.
29. Mariadason JM, Arango D, Corner GA, et al. A gene expression profile that defines colon cell maturation in vitro. Cancer Res 2002;62:4791–804.
30. Bravo SB, Pampin S, Cameselle-Teijeiro J, et al. TGF-beta-induced apoptosis in human thyrocytes is mediated by p27kip1 reduction and is overridden in neoplastic thyrocytes by NF-kappaB activation. Oncogene 2003;22:7819–30.
31. Goswami S, Wang W, Wyckoff JB, Condeelis JS. Breast cancer cells isolated by chemotaxis from primary tumors show increased survival and resistance to chemotherapy. Cancer Res In press 2004.
32. Bailly M, Condeelis J. Cell motility: insights from the backstage. Nat Cell Biol 2002;4:E292–4.
33. Mogilner A, Edelstein-Keshet L. Regulation of actin dynamics in rapidly moving cells: a quantitative analysis. Biophys J 2002;83:1237–58.
34. Loisel TP, Boujemaa R, Pantaloni D, Carlier MF. Reconstitution of actin-based motility of Listeria and Shigella using pure proteins. Nature (Lond) 1999;401:613–6.
35. Ohashi K, Nagata K, Maekawa M, Ishizaki T, Narumiya S, Mizuno K. Rho-associated kinase ROCK activates LIM-kinase 1 by phosphorylation at threonine 508 within the activation loop. J Biol Chem 2000;275:3577–82.
36. Edwards DC, Sanders LC, Bokoch GM, Gill GN. Activation of LIM-kinase by Pak1 couples Rac/Cdc42 GTPase signalling to actin cytoskeletal dynamics. Nat Cell Biol 1999;1:253–9.
37. Cooper JA, Schafer DA. Control of actin assembly and disassembly at filament ends. Curr Opin Cell Biol 2000;12:97–103.
38. Bear JE, Svitkina TM, Krause M, et al. Antagonism between Ena/VASP proteins and actin filament capping regulates fibroblast motility. Cell 2002;109:509–21.
39. Shestakova EA, Singer RH, Condeelis J. The physiological significance of beta-actin mRNA localization in determining cell polarity and directional motility. Proc Natl Acad Sci USA 2001;98:7045–50.
40. Evan GI, Vousden KH. Proliferation, cell cycle and apoptosis in cancer. Nature (Lond) 2001;411:342–8.
41. van 't Veer LJ, Dai H, van de Vijver MJ, et al. Gene expression profiling predicts clinical outcome of breast cancer. Nature (Lond) 2002;415:530–6.
42. Bailly M, Ichetovkin I, Grant W, et al. The F-actin side binding activity of the Arp2/3 complex is essential for actin nucleation and lamellipod extension. Curr Biol 2001;11:620–5.
43. Chan AY, Bailly M, Zebda N, Segall JE, Condeelis JS. Role of cofilin in epidermal growth factor-stimulated actin polymerization and lamellipod protrusion. J Cell Biol 2000;148:531–42.
44. Ghosh M, Song X, Mouneimne G, Sidani M, Lawrence DS, Condeelis JS. Cofilin promotes actin polymerization and defines the direction of cell motility. Science (Wash DC) 2004;304:743–6.
45. Mouneimne G, Soon L, DesMarais V, et al. Phospholipase C and cofilin are required for carcinoma cell directionality in response to EGF stimulation. J Cell Biology 2004;166:697–708.
46. Devreotes P, Janetopoulos C. Eukaryotic chemotaxis: distinctions between directional sensing and polarization. J Biol Chem 2003;278:20445–8.
47. Carlier MF. Control of actin dynamics. Curr Opin Cell Biol 1998;10:45–51.
48. Davila M, Frost AR, Grizzle WE, Chakrabarti R. LIM kinase 1 is essential for the invasive growth of prostate epithelial cells: implications in prostate cancer. J Biol Chem 2003;278:36868–75.
49. Yoshioka K, Foletta V, Bernard O, Itoh K. A role for LIM kinase in cancer invasion. Proc Natl Acad Sci USA 2003;100:7247–52.

50. Zebda N, Bernard O, Bailly M, Welti S, Lawrence DS, Condeelis JS. Phosphorylation of ADF/cofilin abolishes EGF-induced actin nucleation at the leading edge and subsequent lamellipod extension. J Cell Biol 2000;151:1119–28.
51. Sahai E, Olson MF, Marshall CJ. Cross-talk between Ras and Rho signalling pathways in transformation favours proliferation and increased motility. EMBO J 2001;20:755–66.
52. Kamai T, Tsujii T, Arai K, et al. Significant association of Rho/ROCK pathway with invasion and metastasis of bladder cancer. Clin Cancer Res 2003;9:2632–41.
53. Di Modugno F, Bronzi G, Scanlan MJ, et al. Human Mena protein, a serex-defined antigen overexpressed in breast cancer eliciting both humoral and CD8+ T-cell immune response. Int J Cancer 2004;109:909–18.
54. Otsubo T, Iwaya K, Mukai Y, et al. Involvement of Arp2/3 complex in the process of colorectal carcinogenesis. Mod Pathol 2004;17:461–7.
55. Parent CA, Devreotes PN. A cell's sense of direction. Science (Wash DC) 1999;284: 765–70.
56. Iijima M, Huang YE, Devreotes P. Temporal and spatial regulation of chemotaxis. Dev Cell 2002;3:469–78.
57. Yaniv K, Yisraeli JK. The involvement of a conserved family of RNA binding proteins in embryonic development and carcinogenesis. Gene 2002;287:49–54.
58. Tessier CR, Doyle GA, Clark BA, Pitot HC, Ross J. Mammary tumor induction in transgenic mice expressing an RNA-binding protein. Cancer Res 2004;64: 209–14.
59. Herrick DJ, Ross J. The half-life of c-myc mRNA in growing and serum-stimulated cells: influence of the coding and 3′ untranslated regions and role of ribosome translocation. Mol Cell Biol 1994;14:2119–28.